Structure, Spectroscopy, and Spectral Tuning of the Gas-Phase Retinal Chromophore: The β-Ionone "Handle" and Alkyl Group Effect

Alessandro Cembran,[†,‡] Remedios González-Luque,[§] Piero Altoè,[†] Manuela Merchán,*[,§] Fernando Bernardi,[†] Massimo Olivucci,*[,||,⊥] and Marco Garavelli*[,†]

Dipartimento di Chimica "G. Ciamician", Università di Bologna, via Selmi 2, Bologna, I-40126 Italy, Dipartimento di Chimica, Università di Siena, via Aldo Moro, Siena, I-53100 Italy, Centro per lo Studio dei Sistemi Complessi, Via Tommaso Pendola 37, Siena I-53100 Italy, and Departamento de Química Física, Instituto de Ciencia Molecular, Universitat de València, Dr. Moliner 50, Burjassot ES-46100 Valencia, Spain

Received: April 21, 2005; In Final Form: May 26, 2005

The low-lying singlet states (i.e. S_0, S_1, and S_2) of the chromophore of rhodopsin, the protonated Schiff base of 11-*cis*-retinal (**PSB11**), and of its *all-trans* photoproduct have been studied in isolated conditions by using ab initio multiconfigurational second-order perturbation theory. The computed spectroscopic features include the vertical excitation, the band origin, and the fluorescence maximum of both isomers. On the basis of the $S_0 \rightarrow S_1$ vertical excitation, the gas-phase absorption maximum of **PSB11** is predicted to be 545 nm (2.28 eV). Thus, the predicted absorption maximum appears to be closer to that of the rhodopsin pigment (2.48 eV) and considerably red-shifted with respect to that measured in solution (2.82 eV in methanol). In addition, the absorption maxima associated with the blue, green, and red cone visual pigments are tentatively rationalized in terms of the spectral changes computed for **PSB11** structures featuring differently twisted β-ionone rings. More specifically, a blue-shifted absorption maximum is explained in terms of a large twisting of the β-ionone ring (with respect to the main conjugated chain) in the visual S-cone (blue) pigment chromophore. In contrast, the chromophore of the visual L-cone (red) pigment is expected to have a nearly coplanar β-ionone ring yielding a six double bond fully conjugated framework. Finally, the M-cone (green) chromophore is expected to feature a twisting angle between 10 and 60°. The spectroscopic effects of the alkyl substituents on the **PSB11** spectroscopic properties have also been investigated. It is found that they have a not negligible stabilizing effect on the S_1-S_0 energy gap (and, thus, cause a red shift of the absorption maximum) only when the double bond of the β-ionone ring conjugates significantly with the rest of the conjugated chain.

1. Introduction

The visual pigments located in the eye retina are energy transducers. They convert electromagnetic into chemical energy: a process that begins with an ultrafast light-induced cis−trans isomerization of their chromophore (see eq 1) and ends with the excitation of a neuron. In the human eye, the pigments are manufactured and stored in the rod and cone cells. Both rod and cone pigments have the same basic structure: a transmembrane protein called opsin that comprises a retinal prosthetic group bound through a protonated Schiff base linkage. Humans use exclusively the 11-cis protonated Schiff base of retinal (**PSB11**) as chromophore. Rhodopsin (Rh) is the pigment of rods, used in twilight vision. The light absorption of human Rh peaks at 498 nm.[1] The three human cone pigments, used in color vision, peak at 425 nm (S-cone or blue), 530 (M-cone or green), and 560 nm (L-cone or red), where S, M, and L stand for short, medium, and long wavelength.[1,2] The protein structure is similar for the four pigments but differs in the amino acid sequence, and this is usually related to the spectral tuning of the pigments. Indeed, the spectral effects of the substitution of one or more amino acids have been widely investigated.[2−4] In contrast, little is known about the detailed conformation of **PSB11** inside the cone pigments and if this can actually play a role in the tuning of the same spectral properties.

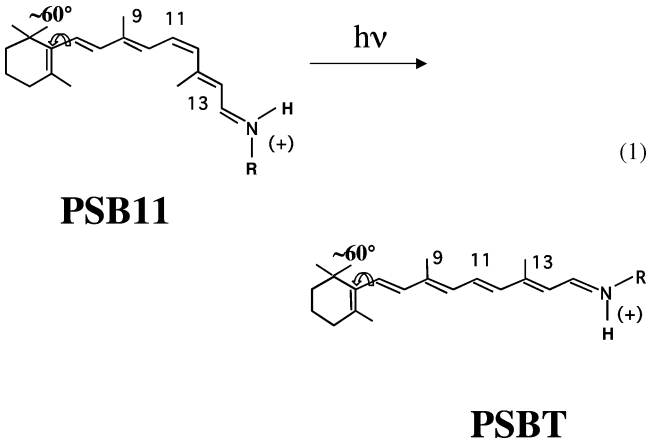

(1)

The availability of a 2.8 Å resolved bovine Rh [5] and its subsequent refinements[6,7] have provided evidence that the β-ionone ring is in a twisted (ca. 60°) 6s-cis conformation inside the protein pocket, confirming that the 11-cis retinal is linked to the ε-amino group of Lys296 as a protonated Schiff base and that Glu113 acts as the counterion. The results of recent quantum mechanics−molecular mechanics (QM/MM) computa-

[†] Università di Bologna.
[‡] Present address: Department of Chemistry and Supercomputing Institute, University of Minnesota, Minneapolis, MN 55455-0431.
[§] Universitat de València.
[||] Università di Siena.
[⊥] Centro per lo Studio dei Sistemi Complessi.

10.1021/jp052068c CCC: $30.25
Published on Web 07/01/2005

tions[8,9] indicates that the presence of a twisted terminal double bond is critical for obtaining a good prediction of the observed absorption maximum of bovine Rh (λ_{max} = 498 nm),[10,11] even if the β-ionone ring of **PSB11** was replaced by a vinyl group.[8] In addition, Andruniow, Ferré, and Olivucci[8,9] concluded that the electrostatic effect of the neutral protein cavity largely counterbalances the blue-shifting effect of the Glu113 counterion on the λ_{max} value. For this reason, as shall be discussed below, the absorption maximum of the full **PSB11** chromophore computed in vacuo is closer to that of Rh rather than to the more blue-shifted λ_{max} observed in solution (e.g. the λ_{max} for **PSB11** in methanol is 442 nm).[12]

In contrast with Rh, the better resolved 1.55 Å X-ray structure[13] of *Halobacterium salinarum* bacteriorhodpsin (bR), a light-driven bacterial proton pump with a longer wavelength (568 nm) absorption maximum,[14] the β-ionone ring is in a 6s-trans conformation and appears to lie substantially in-plane with respect to the rest of the conjugated chain of its *all-trans* retinal chromophore. Thus, speculations may be made that the degree of twisting of the β-ionone ring with respect to the main conjugated chain may serve, among other effects, as a "handle" for tuning the absorption spectra of the chromophore. Such a structural factor may even contribute to establishing the values of the absorption maxima of the three aforementioned blue, red, and green cone pigments.

Here we use ab initio multiconfigurational second-order perturbation theory to investigate the spectral properties of the ground (S_0) and excited states (S_1, S_2) of the visual pigment **PSB11** and its 6s-cis, all-trans photoproduct (**PSBT**) in vacuo (the chromophore is investigated with N being both unsubstituted and substituted by a methyl group (i.e. R $\simeq$ H, Me); see eq 1). Furthermore, we have studied the effect of the twisting of the terminal double bond (i.e. the one comprised in the β-ionone ring), as well as that of the alkyl substituents, on the **PSB11** absorption maximum (simplified models have also been used for this purpose). *Notice that this is the first time that the isolated retinal chromophore is investigated at such a high level of quantum-mechanical theory*. While, currently, there are no experimental data on the gas-phase spectroscopy of these cations, we believe that our calculations, together with past theoretical works,[8,15−19] provide a solid theoretical reference for the understanding of the environmental (e.g. counterion, solvent, and protein cavity) effects of relevance for the biological activity of retinals.[20,21] Also, we hope that the presented results will stimulate further experimental work as modern spectroscopic methods can now be applied to sizable organic gas-phase ions.[22]

2. Theoretical Methods and Computational Details

The ground- and excited-state energies of the considered molecular systems were computed by using multiconfigurational second-order perturbation theory through the CASPT2 method.[23] The successful performance of the CASPT2 approach in computing spectroscopic properties is well-established.[24,25]

The 6-31G* basis set was employed throughout the work. A number of calibration calculations employing larger basis sets of atomic natural orbital (ANO) type show that, for the purpose of the present research, the smaller 6-31G* basis set has enough flexibility. The active space comprises the full π systems, which represents a total of 12 π electrons distributed among 12 π orbitals. The geometry optimizations for the ground and the excited states were performed at the CASSCF(12,12) level.[26] Both single-root and state-average three-roots (weights 1−1−1 for S_0, S_1, and S_2) CASSCF(12,12) calculations were used, yielding similar results.[26] Excitation energies were computed

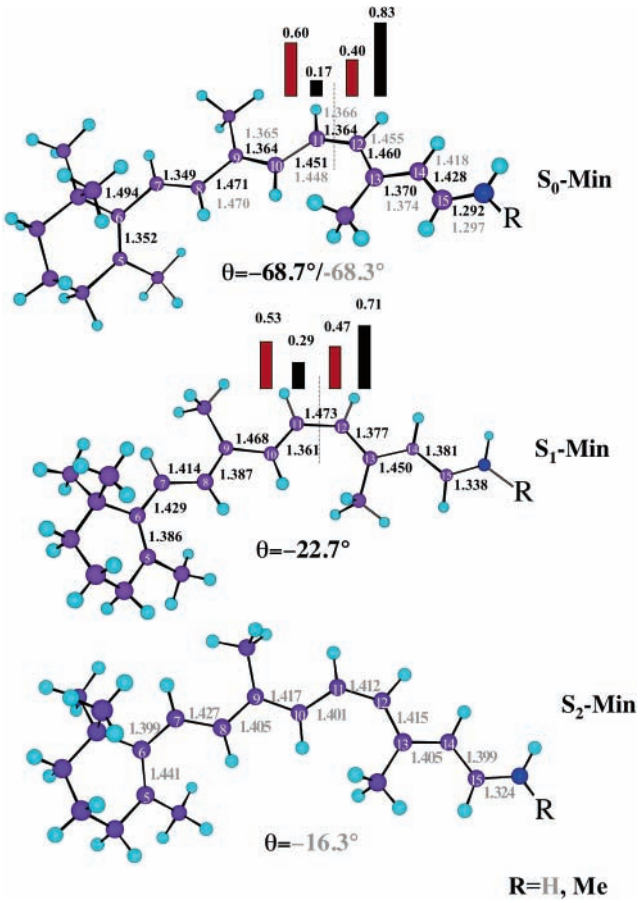

Figure 1. Optimized parameters for S_0 S_1, and S_2 of the **PSB11** system computed at the CASSCF(12,12) level. S_0-Min corresponds to the ground-state minima while S_1-Min and S_2-Min correspond to the S_1 and S_2 excited-state relaxed structures, respectively. The dihedral angle θ is defined by $C_5-C_6-C_7-C_8$. The minus sign indicates that the β-ionone ring is below the polyene chain (i.e. the plane $C_5-C_6-C_7$ is below the plane $C_6-C_7-C_8$).The bar diagrams give the S_0 (black) and S_1 (red) Mulliken charges for the left and right mojeties (the dotted line is the demarcation point) with R = Me.

at the CASPT2//CASSCF/6-31G* level using both single-root and state-average of three roots wave functions. To minimize the influence of weakly interacting intruder states in the state-average PT2 calculations, the so-called imaginary level-shift technique was employed.[27] From calibration calculations, the value of the shift selected was 0.2 au. Unless otherwise stated, all state-average CASPT2 results reported here correspond to that value.

The CASSCF state interaction (CASSI) method[28] was used to calculate the transition dipole moments. In the formula for the oscillator strength the CASSCF transition moment and the energy difference obtained in the CASPT2 computation were used. All calculations were performed with the tools available in the MOLCAS-5 and the Gaussian98 quantum-chemistry softwares.[29,30]

3. Results and Discussion

3.1. PSB11 and PSBT Structures. The main geometrical parameters for the ground and excited states of the **PSB11** and **PSBT** systems are reported in Figure 1 and Figure 2, respectively.

The ground-state equilibrium structure (S_0-Min) of the **PSB11** and **PSBT** cations, display the same basic features. First, bond alternation is the one expected for a ground-state polyene.

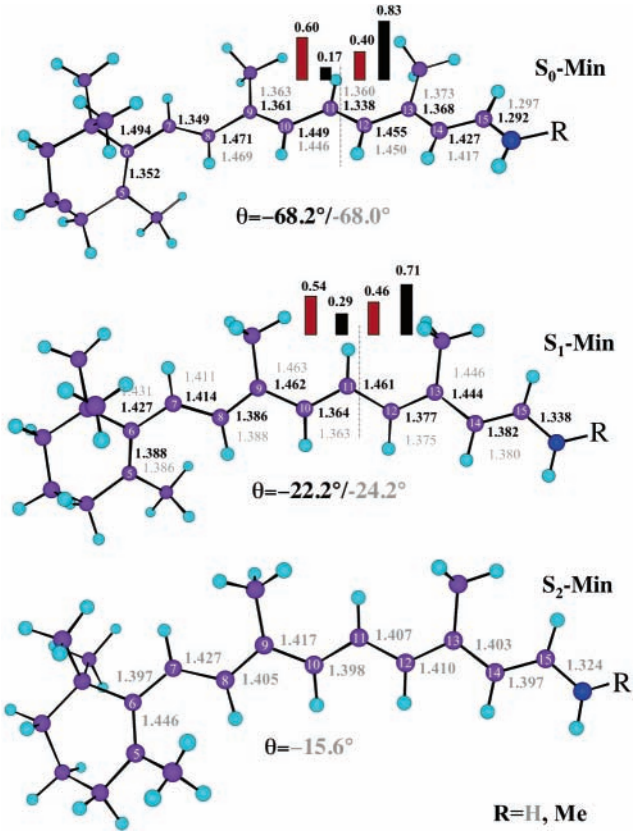

Figure 2. Optimized parameters for S_0, S_1, and S_2 of the **PSBT** system computed at the CASSCF(12,12) level. S_0-Min corresponds to the ground-state minima, while S_1-Min and S_2-Min correspond to the S_1 and S_2 excited-state relaxed structures, respectively. The dihedral angle θ is defined by $C_5-C_6-C_7-C_8$. The minus sign indicates that the β-ionone ring is below the polyene chain (i.e. the plane $C_5-C_6-C_7$ is below the plane $C_6-C_7-C_8$). The bar diagrams give the S_0 (black) and S_1 (red) Mulliken charges for the left and right mojeties (the dotted line is the demarcation point) with R = Me.

Second, the main chain comprising five conjugated double bonds and starting with the Schiff base unit is fully planar, with no twisting about the reactive $C_{11}-C_{12}$ double bond. Most remarkably both structures show in the ground state a highly twisted (a ca. −68° dihedral angle $C_5-C_6-C_7-C_8$ (θ) is computed) 6s-cis β-ionone ring, thus yielding a substantial deconjugation that must have a large effect on the absorption maximum (see the following subsection). Note that this value is quite similar to that observed and computed in Rh. For ground-state **PSB11** the absolute value of the dihedral angle θ, computed at the CASSCF(12,12) level, is larger than those previously obtained by using molecular mechanics, semiempirical, and density functional theory (DFT) schemes, which led to results within the range of 30−50° (see, e.g., ref 18 and references cited therein). Thus, the degree of β-ionone ring twisting seems quite sensitive to the level of calculation. Anyway, on the basis of our experience with polyenes,[31] we believe that the geometrical parameters obtained at the CASSCF(12,12) level reproduce quite well gas-phase data, which have not yet been determined experimentally. Indeed, it is well-documented[31,32] that the inclusion of nondynamic valence π electron correlation by using the π CASSCF wave function (valence π electrons and valence π molecular orbitals (MOs) active) has the trend of making π bonds too long, whereas the treatment of the σ electrons as inactive tends to make σ bonds too short (as in the Hartree−Fock approximation). As a result, the π CASSCF wave function normally leads to experimental accuracy for conjugated hydrocarbons (i.e. the results are close to the well-resolved gas-phase data). The highly twisted conformation in the β-ionone region must be due to important steric interactions between the ring methyl substituents and the chain residues. This is demonstrated by the fact that the structure for the related unsubstituted six double bonds conjugated model **1** (9s-*cis*,4-*cis*-γ-methylundeca-2,4,6,8,10-pentaeniminium cation) has a fully planar conformation in the ground and excited states (see Figure 3).

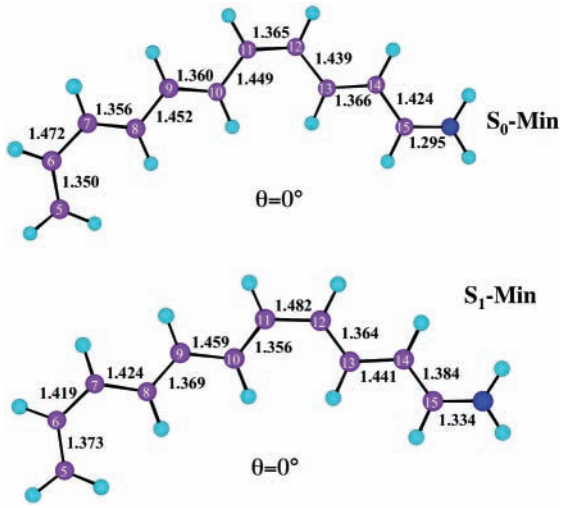

Figure 3. Optimized parameters for S_0 and S_1 of **1** computed at the CASSCF(12,12) level.

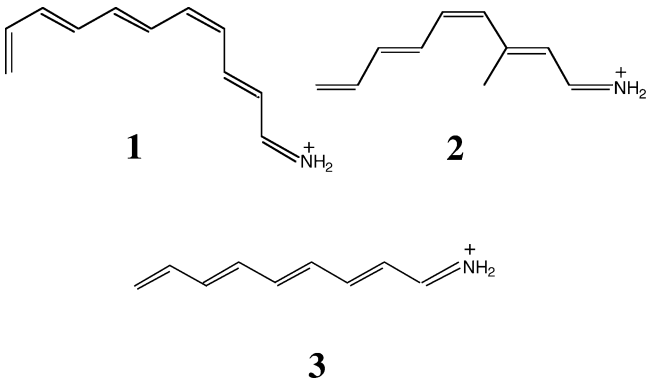

Upon relaxation of the S_0 equilibrium geometry along the S_1 and S_2 energy surfaces, the system equilibrates at two different minima. The S_1 minimum (S_1-Min) displays a bond alternation structure that is substantially reversed with respect to S_0. The single bond/double bond inversion is somehow weaker at the β-ionone ring site where the C_5-C_6 bond gets expanded from 1.35 to 1.39 Å and the adjacent C_6-C_7 single bond gets contracted from 1.49 to 1.43 Å. Most remarkably the β-ionone ring twisting is highly reduced going from ca. −68° to only ca. −22° (Figures 1 and 2). This is, clearly, a consequence of the double bond/single bond inversion that increases the double bond character at C_6-C_7.

The S_1-Min structures are located on a very flat (with respect to the twisting of the central $C_{11}-C_{12}$ double bond) region of the potential energy surface. Because of this, the existence and geometry of true S_1 equilibrium structures depends on the details of the computation. On the other hand, such flatness indicates a facile photoisomerization of the in vacuo chromophore. This is consistent with the almost barrierless S_1 energy profiles computed along the photoisomerization coordinate for the five conjugated double bond models **2** and **3**.[15,16] These computations also show that the initial relaxation from the planar Franck−

Condon (FC) geometry (i.e. from S_0-Min) is dominated by a stretching mode producing the described S_1-Min reversed bond alternation. This relaxation is then followed by a substantially barrierless double-bond twisting, ultimately leading to a twisted conical intersection (CI) between the S_1 and S_0 states.

The S_2 equilibrium structures of **PSB11** and **PSBT** display a different bonding pattern. In this case all bonds residing in the center of the polyene chain have a ca. 1.40−1.41 Å length. The terminal bonds appear to be more expanded with a bond length of about 1.44 Å for the C_5-C_6 bond and 1.32 Å for the $C_{15}-N$ bond. The increased double bond character found at the C_6-C_7 bond is consistent with the further planarization of the β-ionone ring that is now only ca. −16° twisted.

3.2. PSB11 and PSBT Spectroscopy. Wave function analysis establishes that, at S_0-Min, the S_1 state of the $C_{20}H_{30}N^+$ cation, corresponds to the B_u-like (hole-pair) spectroscopic state, while the S_2 state corresponds to the A_g-like (dot−dot) dark state (i.e. the optically allowed excited state S_1 can be related to the $1B_u$ state of polyenes which corresponds, in valence bond terms, to a hole-pair (ionic) excitation, whereas the optically forbidden S_2 state corresponds to the $2A_g$ dot−dot (covalent) excitation). Consistently with the nature of the electronic state, S_1 has a charge-transfer character as it displays the positive charge shifted from the terminal C−N bond toward the β-ionone ring. In contrast, upon photoexcitation to S_2, the charge remains localized in the C−N region and the molecule acquires a biradical character. This results on the full retinal chromophore confirm the previous conclusions derived from the analysis of reduced PSB models such as **2** and **3**.[15] The total and relative energies obtained at the CASSCF(12,12)/6-31G* and CASPT2//CASCF(12,12)/6-31G* levels are reported in Table 1.

The availability of the S_1-Min and S_2-Min equilibrium geometries of **PSB11** and **PSBT** (see above) allow for the computation of the spectral parameters of these gas-phase cations. Here the vertical absorption is assumed to correspond to the observed absorption maximum. The spectral band origin is instead estimated as the energy difference between the excited- and ground-state energies computed at the corresponding optimized geometries. On the other hand, the vertically calculated energy difference from the excited-state minima to S_0 provides a lower bound for the fluorescence maximum. The CASPT2//CASSCF(12,12)/6-31G* computed values for these electronic transitions are compiled in Table 2.

As can be readily seen from the table, the spectroscopic features are similar for both **PSB11** and **PSBT**. For **PSB11** the vertical low-lying electronic transitions are found to be 545 nm (2.28 eV, R = Me) and 355 nm (3.49 eV, R = H) with oscillator strengths of 0.8 and 0.2, respectively. Consistently with previous results for shorter **PSB** models, the S_2 state is placed well above (about 1.2 eV) S_1. This situation is found for all the structures considered in the present work.

Because of the present lack of gas-phase spectroscopic measurements, one is forced to make a comparison with the absorption maximum recorded in solution and in the Rh pigment. While the λ_{max} value for the 11-cis form of the protonated *N*-butylamine Schiff base of retinal in methanol (442 nm, 2.81 eV) and in hexane (458 nm, 2.71 eV) are similar,[12] these differ (ca. 0.5 eV blue-shifted) with respect to our computed gas-phase results (2.28 eV). A possible explanation for the observed blue shift of the band maximum is related to the local effects of the counterion, which are obviously absent in the gas phase. More specifically, the blue shift in solution can be rationalized taking into account the charge distribution in the S_0 and S_1 states. It is established from both the experimental and the theoretical standpoints (see discussion in ref 15) that protonated Schiff bases undergo a large increase in dipole moment in going from the ground state to the S_1 state. At FC the difference in the dipole moment of S_0 and S_1 is computed to be 14.8 D at the CASSCF(12,12) level. In fact, in the ground state the positive charge is localized mainly at the Schiff base nitrogen, whereas it moves toward the opposite side of the molecule in the spectroscopic state. Therefore, the negatively charged counterion (chloride in this case),[11] that is located in proximity of the nitrogen, stabilizes the ground state relative to the spectroscopic state, leading to a blue-shifted absorption maximum (in solution) with respect to the gas phase.

On the other hand, recent accurate QM(CASSCF//CASPT2)/MM(Amber) computations by Andruniow, Ferré, and Olivucci[8,9] for the retinal chromophore in Rh have shown that the effect of the Glu113 counterion is almost fully compensated by the protein cavity, producing an almost gas-phase-like electrostatic environment around the chromophore. It is not surprising, therefore, that the S_1-S_0 gap for the isolated **PSB11** computed here (545 nm, i.e., 2.28 eV) is closer (ca. 0.2 eV difference) to the absorption maximum observed for Rh (498 nm, i.e., 2.49 eV), while a ca. 0.5 eV deviation occurs with respect to solution.

The predicted 545 nm (2.28 eV) absorption maximum for **PSB11** in the gas-phase can be compared to that obtained for the five conjugated double bonds model **2**, 482 nm (2.57 eV), computed at an equivalent level of theory.[15] The nonnegligible red shift seen when comparing **2** to **PSB11** (0.30 eV) can be ascribed to the influence of the β-ionone ring and of the lacking alkyl (i.e. methyl) groups. In fact:

(i) the residual conjugation of the highly twisted sixth double bond of the β-ionone will contribute to red shift the absorption.

(ii) the electron-donating effect of the alkyl substituents in the terminal part of the conjugated chain (i.e. the β-ionone ring skeleton and methyl groups) may stabilize the charge transfer from the N-head to the C-tail of the chromophore, reducing the energy of the S_1 state with respect to the ground state.

It is clear that the extent of twisting of the β-ionone ring may play a major role in tuning the absorption maximum of the different rhodopsin proteins including the rod and cone pigments covering the visible range of the electromagnetic spectrum. More specifically, effects i and ii make retinal a spectrally flexible device that can be tuned between two limits: a red limit provided by six conjugating double bonds (i.e. a fully planar β-ionone ring, as in the bR chromophore) and a blue limit provided by five conjugating double bonds (i.e. a fully twisted and deconjugated β-ionone ring, roughly equivalent to model **2**). (See section 3.3 for a full discussion of this point.)

For the $S_0 \rightarrow S_1$ transition of **PSB11** the band origin is predicted at 1.64 eV with a lower bound for the S_1 fluorescence maximum at 1.40 eV, giving a Stokes shift (computed as the energy difference between vertical absorption and fluorescence maximum) of 0.87 eV. On the other hand, for the $S_0 \rightarrow S_2$ transition of **PSB11** the band origin is predicted at 2.21 eV with a lower bound for the fluorescence maximum at 2.06 eV, giving a large Stokes shift (1.43 eV) as it is typically found for the 2^1A_g excited states of even polyenes, like *all-trans*-1,3,5,7-octatetraene.[31] It is worth mentioning that the possible mechanism for $S_1 \rightarrow S_2$ uphill internal conversion has been recently analyzed for model **1** by Garavelli and co-workers.[19] It was concluded that population of S_2 through relaxation on S_1 is unlikely to happen because of the energy barrier found for reaching the S_1/S_2 intersection seam, supporting a photoisomerization path that fully lies along the charge-transfer S_1 state. Consistently with these findings, at the equilibrium geometry

TABLE 1: CASSCF/6-31G* Absolute and CASPT2/6-31G* Absolute and Relative (ΔE) Energies for S_0, S_1, and S_2 Computed for the Structures Discussed in the Paper[a]

		R = Me			R = H		
structure[b]	state	CASSCF[c] (au)	CASPT2[c] (au)	ΔE, eV (kcal mol^{-1})	CASSCF[d] (au)	CASPT2[d] (au)	ΔE, eV (kcal mol^{-1})
PSB11							
S_0-Min	S_0	−868.19388	−870.88550	0.00 (0.0)	−829.141638	−831.728796	0.00 (0.0)
	S_1	−868.06547	−870.80189	2.28 (52.5)	−829.028907	−831.643530	2.32 (53.5)
	S_2				−828.986299	−831.600605	3.49 (80.5)
S_1-Min	S_0	−868.15537	−870.87671	0.24 (5.5)			
	S_1	−868.08770	−870.82532	1.64 (37.8)			
S_2-Min	S_0				−829.116877	−831.723193	0.15 (3.5)
	S_1				−829.042525	−831.662148	1.81 (41.7)
	S_2				−829.027327	−831.647461	2.21 (51.0)
S_0-Min ($\theta = 0°$)	S_0	−868.18567	−870.88016	0.15 (3.4)			
	S_1	−868.06949	−870.81248	1.99 (45.8)			
S_0-Min ($\theta = -90°$)	S_0	−868.19326	−870.88463	0.03 (0.6)			
	S_1	−868.06364	−870.79953	2.34 (54.0)			
PSBT							
S_0-Min	S_0	−868.20314	−870.89396	0.00 (0.0)	−829.151033	−831.737391	0.00 (0.0)
	S_1	−868.07442	−870.81046	2.27 (52.4)	−829.038116	−831.651947	2.32 (53.5)
	S_2				−828.994923	−831.608279	3.51 (80.9)
S_1-Min	S_0	−868.16633	−870.88614	0.21 (4.9)	−829.126639	−831.732443	0.13 (3.0)
	S_1	−868.09598	−870.83320	1.65 (38.1)	−829.061855	−831.673683	1.73 (39.9)
	S_2				−829.022390	−831.642934	2.57 (59.3)
S_2-Min	S_0				−829.125493	−831.730841	0.17 (3.9)
	S_1				−829.049402	−831.668550	1.87 (43.1)
	S_2				−829.036506	−831.655376	2.23 (51.4)
compd **1**							
S_0-Min	S_0	−479.030311	−480.412333	0.00 (0.0)			
	S_1	−478.921428	−480.331894	2.19 (50.5)			
	S_2	−478.887094	−480.296976	3.14 (72.4)			
S_1-Min	S_0	−479.006484	−480.402138	0.28 (6.4)			
	S_1	−478.941150	−480.338477	2.01 (46.3)			
S_0-Min ($\theta = 45°$)	S_0	−479.024102	−480.401226	0.30 (7.0)			
	S_1	−478.909055	−480.316206	2.61 (60.3)			
	S_2	−478.868616	−480.279678	3.61 (83.3)			
S_1-Min ($\theta = 45°$)	S_0	−478.999464	−480.389527	0.62 (14.3)			
	S_1	−478.926016	−480.320184	2.51 (57.9)			
compd **2**[e]							
S_0-Min	S_0	−441.13038	−442.43089	0.00 (0.00)			
	S_1	−440.99877	−442.33622	2.58 (59.4)			
	S_2	−440.96173	−442.29815	3.61 (83.3)			
S_1-Min	S_0	−441.09848	−442.41879	0.33 (7.6)			
	S_1	−441.01201	−442.34306	2.39 (55.1)			
	S_2	−440.97931	−442.31924	3.04 (70.1)			
S_2-Min	S_0	−441.11066	−442.42283	0.22 (5.06)			
	S_1	−441.00256	−442.33753	2.54 (58.58)			
	S_2	−440.99574	−442.32685	2.83 (65.28)			
compd **3**[f]							
S_0-Min	S_0	−402.0934	−403.3242	0.00 (0.0)			
	S_1	−401.9674	−403.2252	2.69 (62.1)			
	S_2		−403.1888	3.69 (85.0)			
S_1-Min	S_0	−402.0691	−403.3104	0.38 (8.7)			
	S_1	−401.9845	−403.2358	2.41 (55.5)			
	S_2		−403.2014	3.34 (77.1)			

[a] For the sake of comparison, the results on models **2** (see ref 15) and **3** (see ref 16) are also included. [b] When taken frozen during geometry optimization, the sixth double bond rotation is specified (dihedral angle θ $C_5-C_6-C_7-C_8$). [c] Single-state energies. [d] S_0, S_1, and S_2 state average energies (with equal weights). [e] See ref 15. [f] See ref 16.

of S_2, the S_1 state is found to be located 0.4 eV lower in energy at both the CASSCF and CASPT2 levels.

Slightly larger oscillator strengths were found for **PSBT** that features values of 0.9 and 0.2 for the $S_0 \rightarrow S_1$ and $S_0 \rightarrow S_2$ transitions computed at 546 nm (2.27 eV, R = Me) and 353 nm (3.51 eV, R = H), respectively. The predicted band origins are 1.73 (S_1) and 2.23 eV (S_2), and the fluorescence maxima (a lower bound) are computed to be 1.60 (S_1) and 2.05 eV (S_2). The experimental λ_{max} for the all-trans protonated *N*-butylamine retinal Schiff base is 445 nm (2.79 eV) in methanol and 458 nm (2.71 eV) in hexane.[12] The experimental fluorescence has λ_{max} values of 675 nm (1.84 eV) in methanol and 620 nm (2.0 eV) in hexane.[33] Therefore, the observed spectral paramenters in solution have large (blue-shift) deviations with respect to the results predicted in the gas phase. Again, we believe that this disagreement is due to the effects of the counterion as also confirmed by the successful computations of the absorption and emission maxima for **PSB11** in solution.[8,9]

From the CASSCF transition moments and the CASPT2 energies, the radiative lifetimes (τ_{rad}) for fluorescence have been obtained by using the Strickler−Berg relationship.[34] The theoretically derived results for S_1 and S_2 of **PSBT** are 11.7 and 44 ns, respectively, consistent with the mainly B_u- and A_g-like character of the electronic states. For S_1 this value is consistent with the experiment for the *N*-butylamine Schiff base of retinal in hexane (less than 27 ns).[33] Furthermore, assuming

TABLE 2: Computed CASPT2//CASSCF(12,12)/6-31G* Vertical, Adiabatic, and Fluorescence Electronic Transitions for the Low-lying Excited States (S_1 and S_2) of the Full Chromophores PSB11 and PSBT and of the Model Chromophores 1, 2 and 3[a]

		R = Me			R = H		
structure	state	abs (vertical)	adiabatic(0−0)	emission (vertical)	abs (vertical)	adiabatic(0−0)	emission (vertical)
PSB11[b]	S_1	545 (2.27) $f = 0.8$	756 (1.64)	886 (1.40) $f \simeq 0.7$	534 (2.32) $f \simeq 1.0$		
	S_2				355 (3.49) $f \simeq 0.2$	560 (2.21)	602 (2.06)
PSB11($\theta = 0°$)	S_1	673 (1.84)					
PSB11($\theta = -90°$)	S_1	535 (2.31)					
PSBT	S_1	546 (2.27) $f \simeq 0.9$	752 (1.65)	862 (1.44) $f \simeq 1.1$	533 (2.33) $f \simeq 1.1$	715 (1.73)	775 (1.60)
	S_2				353 (3.51) $f \simeq 0.2$	556 (2.23)	604 (2.05)
compd **1**	S_1	566 (2.19)	617 (2.01)	717 (1.73)			
	S_2	395 (3.14)					
compd **1**($\theta = 45°$)	S_1	537 (2.31)	561 (2.21)	656 (1.89)			
	S_2	375 (3.31)					
compd **2**[c]	S_1	482 (2.57)	519 (2.39)	602 (2.06)			
	S_2	344 (3.61)	438 (2.83)	475 (2.61)			
compd **3**[d]	S_1	461 (2.69)	515 (2.41)	611 (2.03)			
	S_2	336 (3.69)					

[a] Wavelengths are given in nm. Energies are given in eV (within parentheses). Where computed, the oscillator strength *f* is also reported. For the sake of comparison, the results on model **2** (see ref 15) and **3** (see ref 16) are also included. [b] When taken frozen during geometry optimization, the sixth double bond rotation is specified (dihedral angle θ $C_5-C_6-C_7-C_8$). [c] See ref 15. [d] See ref 16.

a fluorescence quantum yield of 1.8×10^{-4} (as in hexane), the computed intrinsic fluorescence lifetime leads to 2 ps in reasonable agreement with the measured value (less than 5 ps).[33]

The change in S_0-S_1 and S_1-S_2 energy gaps of **PSB11** and **PSBT** as a function of the equilibrium geometry is documented in Table 1. Wave function analysis indicates that, upon either S_1 or S_2 relaxation, there is *no change in the order of the electronic states*. So, in the isolated cation of both isomers, S_1 remains the spectroscopic state even at the equilibrium geometry of the dark state S_2. On the other hand, the S_1-S_2 energy gap of **PSBT** is reduced from 1.19 to 0.84 eV when passing from the S_0 to the S_1 equilibrium structure and from 0.84 to 0.36 eV when shifting to the S_2 equilibrium structure.

3.3. Spectroscopic Effects of the Twisting of the β-Ionone Ring. In this section we focus on the relationship between the conformation of the β-ionone ring and the spectroscopic properties of gas-phase **PSB11**. We show that the extent of the β-ionone twisting determines the absorption maximum of the chromophore and may therefore be exploited to tune its sensitivity to a given color.

As discussed above in section 3.2, the fact that **PSB11** absorbs at 458 nm (2.71 eV) in hexane and at 498 nm (2.49 eV) in Rh is explained with the idea that the cavity amino acid partial charges counterbalance the counterion charge. However, the protein cavity of the cone (color) pigments is capable of tuning the absorption maximum of the retinal chromophore over a wide spectral range, going from 360 to 635 nm in vertebrates. This may be due to specific amino acid substitutions with respect to Rh. For instance, those persons who possess a 557 nm L-cone pigment have serine at position 180, while those with a 552 nm pigment have alanine.[35] Therefore, the difference between the pigments (i.e. the spectral tuning) could be ultimately related to the interactions of these amino acids with the chromophore. For a long time this was assumed to be the case and that spectral tuning was mainly due to the presence of different charged residues in the protein cavity. However, it has now been established that the opsin pocket, where the chromophore is tightly held, is electrically neutral.[36] Four years ago, Sakmar, Mathies, and co-workers proposed that long-range molecular interactions tune the wavelength of the photons captured by the photoreceptors.[4] In fact, through a detailed analyses of resonance Raman spectra of several visual pigments, it was concluded that the spectral tuning is not determined by the local perturbations of the chromophore structure imposed by the protein cavity but to the extent of the delocalized electronic structure of the chromophore, which was monitored through the changes of the ethylenic mode. In fact, the red pigment absorption maximum has a chromophore showing a longer delocalized structure than that of the blue pigment.[4] In terms of the molecular structure of **PSB11** the following questions arise: What is the meaning of the more delocalized electronic structure? What geometry changes are undertaken to fulfill such requirement?

From simple MO arguments, and consistently with the computational results on model systems, the extent of delocalization primarily increases as a function of the planarization of the β-ionone ring with respect to the rest of the polyene chain. Indeed (see Table 2), the computed lowest transition energy for the 4-*cis*-γ-9s-*cis*-undeca-2,4,6,8,10-pentaeniminium cation **1** at two different $C_8-C_9-C_{10}-C_{11}$ dihedral angles $\theta = 0°$ (S_0-Min) and $\theta = 45°$ (simulating the twisting of the omitted β-ionone ring) are 2.19 and 2.31 eV, yielding a 0.12 eV blue shift. An additional blue shift is expected upon further increasing of the ring torsion, for instance, going from model **1** ($\theta = 45°$) to model **2**, which roughly approximates a fully twisted (i.e. $\theta = 90°$) model **1**, where the sixth double bond does not conjugate. The same reasoning can be applied to the absorptions of **PSB11** computed at different degrees of twisting of the β-ionone ring. Indeed, an increasing blue shift is computed on going from the planar conformer ($\theta = 0°$, 673 nm), to the twisted ground-state minimum ($\theta = -68°$, 545 nm), to the fully deconjugated ($\theta = -90°$, 535 nm) structure (see Table 2). Thus, the general conclusion is that upon increasing the twisting angle of the terminal double bond (i.e. of the β-ionone ring in **PSB11**), a progressive blue shift occurs in the computed λ_{max}. In other words, the results of Table 2 suggest the idea that the value of θ in the **PSB11** chromophore decreases on going from the S- to the L-cone pigments. This prediction implies that in the protein pocket the θ value in the blue pigment (425 nm) should be larger than θ in Rh (498 nm) and that θ in Rh should be larger than the θ values of the green (530 nm) and red pigments (560 nm). Since it is known that in Rh the twisting angle is of ca. 60° (i.e. very similar to the optimized gas-phase value), it

can also be anticipated that the β-ionone ring in the S-cones could become somewhat larger than 60°. However, it must be noticed that even with a fully deconjugated ($\theta = -90°$) ring the isolated **PSB11** chromophore would not feature the right blue shift ($\lambda_{max} = 535$ nm). Indeed, already at the ground-state minimum ($\theta = -68°$, $\lambda_{max} = 545$ nm) the ring can be considered as being almost fully deconjugated. It is therefore apparent that other environment-dependent structural and/or electrostatic effects must be responsible for the ca. 100 nm difference between the blue pigment absorption and the fully twisted **PSB11**.

At this point we may formulate a tentative relationship between the β-ionone ring twisting and the observed spectral tuning. Assuming that the calculated absorption shifts on twisting the ionone ring of the isolated **PSB11** chromophore can be transferred to the three cone pigments, we may predict a fully twisted ($\theta = -90°$) and fully coplanar ($\theta = 0°$ retinal for the S-cone and L-cone pigments and a chromophore twisted in the 60−10° range for the M-cone pigment). Indeed, the **PSB11** gas-phase absorption computed for the fully twisted (535 nm) and the coplanar (673 nm) ring roughly features the same shift observed for the S-cone (425 nm) and L-cone (560 nm) pigments. For the same reasoning, a chromophore twisted in the 60−10° range is expected for the M-cone pigment.

From this particular point of view the **PSB11** system becomes the main player in the visual tuning and the specific protein pocket makes the work of selecting a particular conformation. With no doubt, color vision enables a better adaptation to the environment and must have played an important role in the evolution of vertebrates introducing much more effective adaptive tools with respect to the black-and-white vision. This argument stimulates our interest for understanding the photochemical behavior of other biological systems where the presence of the retinal chromophore has been demonstrated. For instance, the light-sensitive pigment melanopsin found in the skin[37] and a large variety of challenging retinal-based photoreceptors, which most probably are related with circadian and photoperiodic physiology.[38]

3.4. Spectroscopic Effects of the Alkyl Substitution. In the previous section we have mentioned that **2** provides a model for a fully twisted (i.e. $\theta = -90°$) **PSB11** chromophore where the sixth double bond does not conjugate with the remaining part of the π system. The electron-donating effects of the alkyl (β-ionone ring and methyl groups) substituents, not accounted for in **2**, can be evaluated by comparing the S_1-S_0 energy gaps (see Tables 1 and 2) of **2** (482 nm) with that of the fully twisted ($\theta \simeq -90°$) **PSB11** (535 nm). Accordingly, a significant 47 nm (0.25 eV) red shift is predicted which can be fully assigned to the inductive effect of the ring and the methyl groups (more precisely, the transition computed for **2** can be seen as an upper bound of the absorption maximum of model **1** and **PSB11** both at −90°). Of course, a simple explanation of these effects can be provided on the basis of the fact that alkyl groups stabilize the positive charges. Since, upon photoexcitation, the chromophore positive charge is partially transferred from the N-head to the C-tail of the chain the alkyl groups should facilitate this process by stabilizing the positive charge translocation. These computations have allowed unambiguous evaluation of such a contribution in the stability of the excited state of retinal chromophores.

To further explore this effect and to determine how much the β-ionone ring frame and methyl substituents contribute to the positive charge stabilization, the optimized S_0-Min and the S_1-Min structures of **PSB11** have been further investigated. To this purpose, four model structures (**a**, **a′**, **b**, **b′**; see Chart 1) have been built starting form these minima. The models have exactly the same molecular geometry of S_0-Min (**a** and **b**) and S_1-Min (**a′** and **b′**) except for a set of bonds that have been broken and saturated with hydrogens.[39] In particular, while **a** and **a′** lack only part of the β-ionone ring, **b** and **b′** lack all the alkyl substituents yielding model **1** defined above.

CHART 1

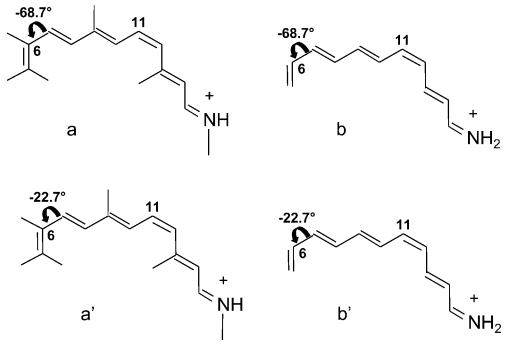

TABLE 3: Computed CASPT2//CASSCF(12,12)/6-31G* Vertical, Adiabatic, and Fluorescence Electronic Transitions for the Low-Lying Excited State S_1 of the Molecular Structures a/a′ and b/b′ [a]

structure	state	abs (vertical)	adiabatic (0−0)	emission (vertical)
a/**a**	S_1	542 (2.29) $f = 0.8$	743 (1.67)	861 (1.44) $f = 0.7$
b/**b** (model **1**)	S_1	553 (2.24) $f = 1.0$	926 (1.34)	751 (1.65) $f = 1.1$

[a] Wavelengths are given in nm. Energies are given in eV (within parentheses). Where computed, the oscillator strength *f* is also reported.

To rationalize the effects of the alkyl groups on the excited-state stability, we assume that the *steric* effects of the removed groups are the same in all the electronic states. Table 3 reports the spectroscopic data (i.e. absorption energy, emission, and oscillator strength) of the four models. It is useful to compare the S_0-S_1 energy gaps with those of the corresponding **PSB11** molecular structures (i.e. S_0-Min and S_1-Min) reported in Table 2. Strikingly, **a** and **a′** reproduce the energy gap within 1 kcal mol^{-1} for both S_0-Min and S_1-Min. On the other hand, while **b** reproduce the energy gap seen at S_0-Min, **b′** overestimates the energy gap of S_1-Min by ca. 5 kcal mol^{-1}. Concurrently, it is worth noting that planar **1** ($\theta = 0°$, $\lambda_{max} = 567$ nm) does not reproduce the absorption of the corresponding planar **PSB11** chromophore ($\theta = 0°$, $\lambda_{max} = 670$ nm).

The computed pattern of S_0-S_1 energy gap changes are readily explained on the basis of the electron-donating effect of the alkyl groups that facilitate the charge transfer occurring upon excitation to S_1. In fact, *provided the sixth double bond is fully conjugating with the rest of the chain* (i.e. the backbone is planar or almost planar), the alkyl groups will stabilize the S_1 charge-transfer state with respect to S_0 as the positive charge is allowed to migrate on the terminal double bond (there are three alkyl groups directly connected to the sixth double bond in **PSB11** or **a**/**a′**). This will surely happen at the planar ($\theta = 0°$) structures **1** and **PSB11** as well as at the optimized S_1-Min point of **PSB11** (where an almost planar β-ionone ring exists with θ ca. 20°), thus, at **a′** and **b′**. However, this will not happen at the S_0-Min point of **PSB11** where the sixth double bond, bearing the majority of the alkyl groups, is almost fully twisted ($\theta = -68°$). In fact, in this case, the deconjugated sixth double bond does not allow the positive charge to flow close to the alkyls.

Notice that the fact that the S_1 stabilization due to the alkyl groups is important in fully conjugated chromophores implies that model **1** (i.e. **b′**) will be a quantitatively not correct model for a nearly planar **PSB11**. In other words, due to the lack of alkyl substituents on the sixth double bond (i.e. the β-ionone double bond), **1** will not be able to reproduce good spectra yielding a blue-shifted absorption (2.19 eV, i.e., 567 nm) when compared to the corresponding planar ($\theta = 0°$) **PSB11** (670 nm). Exactly the same effect explains the blue-shifted emission (see Tables 2 and 3) observed for **b′** (751 nm) and for the S_1-Min of **1** (720 nm) with respect to the S_1-Min of **PSB11** (870 nm). Finally, Mulliken charges analysis (see Supporting Information, Table SI2) reveal that both **a** (**a′**) and **b** (**b′**) provide an accurate description of the charge translocation occurring upon excitation as compared to more realistic models (see Figures 1 and 2). In summary, it can be affirmed that, in general, the alkyl groups are necessary for a quantitative description of the transition energies.

4. Summary and Conclusions

Ab initio CASPT2//CASSCF computations have been performed for the *unreduced* **PSB11** retinal chromophore in its ground and lowest lying excited states. Thus, the present work reports the first high-level quantum chemical investigation for the real Rh chromophore in *isolated conditions*.

Among other results we have provided evidence that **PSB11** and **PSBT** feature a severely and moderately twisted β-ionone ring when taken in their ground state (S_0) and transient excited states (S_1 and S_2), respectively. The spectroscopic features, at the ground- and excited-state optimized points, have been computed and the effect of the β-ionone ring twisting on the photophysical properties has been evaluated and compared to the spectral features of the visual pigments (i.e. Rh and the S(blue), M(green), and L(red) cone pigments responsible for color vision). On the basis of our results and of the available experimental data a working hypothesis has been presented that implies that the extent of the β-ionone ring twisting allows for the spectral tuning of the retinal chromophore. According to this hypothesis, the protein environment (namely, the nearby amino acids) would force the β-ionone ring into the specific conformation required for responding to a given wavelength. In particular, the β-ionone ring is made more and more coplanar with the polyene chain to respond to longer and longer wavelengths. Thus, twisting the ionone ring of the isolated protonated Schiff of retinal can account for a large part of the spectral shift of the visual pigments: the β-ionone ring of the S-cone chromophore would be fully twisted, the one of the L-cone chromophore coplanar while the chromophore of the green M-cone pigment would be slightly twisted (with a value on between 10 and 60°). It is, however, clear that extra effects related to the protein have to be taken into account explicitly in order to rationalize the absorbance maximum of these pigments in the UV range (360 nm).

Finally, it has been shown that the alkyl substituents are required to reproduce quantitatively the transition energies (the description provided by the simplified model **a** (**a′**) is sufficient to account for a *quantitative* description of the energy gaps). Thus simplified **PSB11** models such as **1** and **2** may not be accurate enough. The computed alkyl group effect has been rationalized and has been shown to be crucial for coplanar conformations (e.g. $\theta = 0°$ or S_1-Min structures) or the β-ionone ring.

Although the spectroscopic data presented above can only be compared with gas-phase spectral data, we hope they provide a solid reference for the understanding of the environmental effects (e.g. the counterion, solvent, and protein cavity effects), complementing the experimental investigation on these biologically relevant chromophores.[20,21] We also hope that the presented results will stimulate further experimental work as modern spectroscopic methods can be applied to sizable organic ions in the gas phase.

Acknowledgment. Financial support through Projects BQU2001-2926 and CTQ2004-01739 from the Spanish Ministerio de Ciencia y Tecnología (MCyT) and by the Generalitat Valenciana is gratefully acknowledged. M.G. is grateful to the University of Bologna (Funds for Selected Research Topics), MIUR (grant 60%), MURST Cofin 2003 (Projects: "Reazioni stereoselettive promosse da nuovi sistemi catalitici e loro modellistica"), and FIRB 2001 (Grant RBAU01L2HT). We wish to thank CINECA for granted calculation time on their computers. M.O. is also grateful for a FIRB grant (RBAU01EPMR).

Supporting Information Available: Tables including energies for a/a' and b/b' and Mulliken charges analysis. Two additional figures. Cartesian coordinates of all the structures discussed in the text. This material is available free of charge via the Internet at http://pubs.acs.org.

References and Notes

(1) Wald, G.; Brown, P. K. *Science* **1958**, *127*, 222.
(2) McBee, J. K.; Palczewski, K.; Baehr, W.; Pepperberg, D. R. Confronting Complexity: The Interlink of Phototransduction and Retinoid Metabolism in Vertebrate Retina. In *Progress in Retinal and Eye Research*; Elsevier: Oxford, Great Britain, 2001; Vol. 20, p 469.
(3) Nathans, J.; Piantanida, T. P.; Eddy, R. L.; Shows, T. B.; Hogness, D. S. *Science* **1986**, *232*, 203.
(4) Kochendoerfer, G. G.; Lin, S. W.; Sakmar, T. P.; Mathies, R. A. *Trends Biochem. Sci.* **1999**, *24*, 300.
(5) Palczewski, K.; Kumasaka, T.; Hori, T.; Behnke, C. A.; Motoshima, H.; Fox, B. A.; Le Trong, I.; Teller, D. C.; Okada, T.; Stenkamp, R. E.; Yamamoto, M.; Miyano, M. *Science* **2000**, *289*, 739.
(6) Teller, D. C.; Okada, T.; Behnke, C. A.; Palczewski, K.; Stenkamp, R. E. *Biochemistry* **2001**, *40*, 7761.
(7) Okada, T.; Fujiyoshi, Y.; Silow, M.; Navarro, J.; Landau, E. M.; Shichida, Y. *Proc. Natl. Acad. Sci. U.S.A.* **2002**, *99*, 5982.
(8) Ferré, N.; Olivucci, M. *J. Am. Chem. Soc.* **2003**, *125*, 6868.
(9) Andruniów, T.; Ferré, N.; Olivucci, M. *Proc. Natl. Acad. Sci. U.S.A.* **2004**, *101*, 17908.
(10) Mathies, R.; Lugtenburg, J. The Primary Photoreaction of Rhodopsin. In *Molecular Mechanism of Vision*; Stavenga, D. G., DeGrip, W. J., Pugh, E. N. J., Eds.; Elsevier Science Press: New York, 2000; Vol. 3, p 55.
(11) Kandori, H.; Shichida, Y.; Yoshizawa, T. *Biochemistry (Moscow)* **2001**, *66*, 1197.
(12) Freedman, K. A.; Becker, R. S. *J. Am. Chem. Soc.* **1986**, *108*, 1245.
(13) Luecke, H.; Schobert, B.; Richter, H. T.; Cartailler, J. P.; Lanyi, J. *J. Mol. Biol.* **1999**, 899.
(14) Rehorek, M.; Heyn, M. P. *Biochemistry* **1979**, *18*, 4977.
(15) González-Luque, R.; Garavelli, M.; Bernardi, F.; Merchán, M.; Robb, M. A.; Olivucci, M. *Proc. Natl. Acad. Sci. U.S.A.* **2000**, *97*, 9379.
(16) De Vico, L.; Page, C. S.; Garavelli, M.; Bernardi, F.; Basosi, R.; Olivucci, M. *J. Am. Chem. Soc.* **2002**, *124*, 4124.
(17) Ben-Nun, M.; Molnar, F.; Schulten, K.; Martinez, T. J. *Proc. Natl. Acad. Sci. U.S.A.* **2002**, *99*, 1769.
(18) Schreiber, M.; Buss, V.; Sugihara, M. *J. Chem. Phys.* **2003**, *119*, 12045.
(19) Cembran, A.; Bernardi, F.; Olivucci, M.; Garavelli, M. *J. Am. Chem. Soc.* **2003**, *125*, 12509.
(20) Okada, T.; Emst, O. P.; Palczewski, K.; Hofmann, K. P. *Trends Biochem. Sci.* **2001**, *26*, 318.
(21) Horst, M. A. v.; Hellingwerf, K. J. *Acc. Chem. Res.* **2004**, *37*, 13.
(22) Nielsen, S. B.; Lapierre, A.; Andersen, J. U.; Pedersen, U. V.; Tomita, S.; Andersen, L. H. *Phys. Rev. Lett.* **2001**, *22*, 228102.
(23) Andersson, K.; Malmqvist, P.-Å.; Roos, B. O. *J. Chem. Phys.* **1992**, *96*, 1218.
(24) Roos, B. O.; Andersson, K.; Fulscher, M. P.; Malmqvist, P.-Å.; Serrano-Andrés, L.; Pierloot, K.; Merchán, M. *Adv. Chem. Phys.* **1996**, *93*, 219.

(25) Merchán, M.; Serrano-Andrés, L.; Fulscher, M. P.; Roos, B. O. In *Multiconfigurational Perturbation Theory Applied to Excited States of Organic Compounds*; Hirao, K., Ed.; World Scientific: Amsterdam, 1999; Vol. 4, p 161.

(26) *Ab Initio Methods in Quantum Chemistry*—II; John Wiley & Sons: New York, 1987.

(27) Forsberg, N.; Malmqvist, P.-Å. *Chem. Phys. Lett.* **1997**, *274*, 196.

(28) Malmqvist, P.-Å.; Roos, B. O. *Chem. Phys. Lett.* **1989**, *155*, 189.

(29) Andersson, K.; Blomberg, M. R. A.; Fülscher, M. P.; Karlström, G.; Lindh, R.; Malmqvist, P.-Å.; Neogrády, P.; Olsen, J.; Roos, B. O.; Sadlej, A. J.; Schütz, M.; Seijo, L.; Serrano-Andrés, L.; Siegbahn, P. E. M.; Widmark, P.-O. *MOLCAS*, 5.0 ed.; Lund University: Lund, Sweden, 1999.

(30) Frisch, M. J.; Trucks, G. W.; Schlegel, H. B.; Scuseria, G. E.; Robb, M. A.; Cheeseman, J. R.; Zakrzewski, V. G.; Montgomery, J. A., Jr.; Stratmann, R. E.; Burant, J. C.; Dapprich, S.; Millam, J. M.; Daniels, A. D.; Kudin, K. N.; Strain, M. C.; Farkas, O.; Tomasi, J.; Barone, V.; Cossi, M.; Cammi, R.; Menucci, B.; Pomelli, C.; Adamo, C.; Clifford, S.; Ochterski, J.; Petersson, G. A.; Ayala, P. Y.; Cui, Q.; Morokuma, K.; Malick, D. K.; Rabuck, A. D.; Raghavachari, K.; Foresman, J. B.; Cioslowski, J.; Ortiz, J. V.; Stefanov, B. B.; Liu, G.; Liashenko, A.; Piskorz, P.; Komaromi, I.; Gomperts, R.; Martin, R. L.; Fox, D. J.; Keith, T.; Al-Laham, M. A.; Peng, C. Y.; Nanayakkara, A.; Gonzalez, C.; Challacombe, M.; Gill, P. M. W.; Johnson, B. G.; Chen, W.; Wong, M. W.; Andres, J. L.; Gonzalez, C.; Head-Gordon, M.; Replogle, E. S.; Pople, J. A. *Gaussian 98*, Revision A.6 ed.; Gaussian Inc.: Pittsburgh, PA, 1998.

(31) Serrano-Andrés, L.; Lindh, R.; Roos, B. O.; Merchán, M. *J. Phys. Chem.* **1993**, *97*, 9360.

(32) Page, C. S.; Olivucci, M.; Merchán, M. *J. Phys. Chem.* **2000**, *104*, 8796.

(33) Bachilo, S. M.; Bondarev, S. L.; Gillbro, T. *J. Photochem. Photobiol., B* **1996**, *34*, 39.

(34) Strickler, S. M.; Berg, R. A. *J. Chem. Phys.* **1962**, *37*, 814.

(35) *Photobiology: The Science of Light and Life*; Kluwer Academic: Dordrecht, The Netherlands, 2002.

(36) Fahmy, K.; Jager, F.; Beck, M.; Zvyaga, T. A.; Sakmar, T. P.; Siebert, F. *Proc. Natl. Acad. Sci. U.S.A.* **1993**, *90*, 10206.

(37) Provencio, I.; Jiang, G.; Grip, W. J. d.; Hayes, W. P.; Rollag, M. D. *Proc. Natl. Acad. Sci. U.S.A.* **1998**, *95*, 340.

(38) Foster, R. G.; Soni, B. G. *Rev. Reprod.* **1998**, *3*, 145.

(39) Hydrogen atoms have been placed along the same bonds which were connecting the cut carbon atoms. Reasonable bond distances have been chosen for the hydrogen atoms: 1.083 Å for **a**/**a′**; 1.076 Å for the hydrogen connected to carbon atoms and 1.036 Å for that connected to the nitrogen atom in **b**/**b′**.